Characterizing the Dose Response of Hyperoxia with Brain Perfusion

Elizabeth G. Damato; Seth J. Fillioe; Ian S. Vannix; Lily K. Norton; Seunghee P. Margevicius; Jessica L. Beebe; Michael J. Decker

BACKGROUND: Tactical aviators require administration of enhanced inspired oxygen concentrations (hyperoxia) to reduce risk of hypobaric hypoxia and decompression injuries. Hyperoxia is not without consequence; it reduces cerebral perfusion (CBF). Characterizing the relationship between F_IO_2 and CBF is necessary to establish F_IO_2 levels that do not reduce CBF yet are sufficient to mitigate risk of in-flight physiological stressors. To achieve that goal, this study's objective was to determine whether a dose-response relationship exists between F_IO_2 and CBF and, if so, the F_IO_2 at which CBF significantly declines.

METHODS: Healthy male and female subjects ($N = 26$) were randomized to receive either low dose F_IO_2 of 30%, 40%, 50%, and 100% (Arm 1) or high dose F_IO_2 of 60%, 70%, 80%, and 100% (Arm 2), followed by a return to 21% for both groups. Subjects were placed within a 3-Tesla MRI scanner equipped with pseudocontinuous arterial spin labeling software (pCASL) to measure CBF. Baseline CBF measurements were obtained during exposure to 21% F_IO_2, with subsequent CBF measurements obtained at each predetermined F_IO_2 level.

RESULTS: Baseline CBF did not differ between subjects in Arm 1 and Arm 2. Low dose $F_IO_2 \leq 50\%$ did not affect CBF. In contrast, high dose $F_IO_2 \geq 60\%$ significantly reduced CBF. Exposure to 100% F_IO_2 led to similar reductions of CBF for subjects in both Arm 1 and Arm 2.

DISCUSSION: The neurovascular system appears to respond to increasing F_IO_2 levels in a dose dependent manner, with significant reductions in CBF with F_IO_2 exposures ≥ 60%.

KEYWORDS: hyperoxia, tactical aviation, cerebral perfusion, magnetic resonance imaging, arterial spin labeling.

Damato EG, Fillioe SJ, Vannix IS, Norton LK, Margevicius SP, Beebe JL, Decker MJ. *Characterizing the dose response of hyperoxia with brain perfusion*. Aerosp Med Hum Perform. 2022; 93(6):493–498.

Tactical aviation is accompanied by risks of environmental hypoxia, venous gas emboli, and decompression sickness.[12] Initial manifestations may include tingling in the extremities, diminished manual dexterity, and clumsiness or disorientation which may not be self-evident.[2,14,18] Without prompt recognition and intervention, these symptoms can rapidly progress into acute and severe cognitive impairment, and, potentially, a catastrophic event.[17] Neuroprotection against those hazards is conferred by providing a continuous fraction of inspired oxygen (F_IO_2) between 35–100% (hyperoxia). However, administration of hyperoxic gas mixtures is not without consequence; an F_IO_2 of 100% leads to a significant drop in cerebral perfusion (CBF).[1,3,9]

Adequate CBF is necessary to sustain central nervous system integrity and cognitive performance.[10] Our recent study revealed that 100% F_IO_2 reduced CBF by 35%.[1] Physiological outcomes included reduced oxygen delivery to the brain, changes in cortical electrical activity (EEG) during cognitive testing, and diminished heart and respiratory rates. Those outcomes raised new questions of: 1) whether a dose-response relationship exists between F_IO_2 and CBF; and 2) whether CBF remains attenuated upon cessation of hyperoxia. That critical

From the Naval Medical Research Unit-Dayton, Dayton, OH, USA; Case Western Reserve University School of Medicine, Cleveland, OH, USA; Jacobs School of Medicine and Biomedical Sciences, University at Buffalo, Buffalo, NY, USA; and The Wright Center Graduate Medical Education, HealthSource of Ohio, New Richmond, OH, USA.

This manuscript was received for review in January 2022. It was accepted for publication in March 2022.

Address correspondence to: Michael J. Decker, Ph.D., Case Western Reserve University School of Medicine, Cleveland, OH, USA; mjd6@case.edu.

DOI: https://doi.org/10.3357/AMHP.6056.2022

knowledge gap impedes development of oxygen delivery schedules aimed at mitigating the risk of hypoxia without concomitantly reducing CBF. Any mechanism reducing CBF could potentially confer vulnerability toward hypergravity-induced brain hypoperfusion followed by a loss of consciousness.

To inform our understanding of the neurovascular system's functional response to a range of hyperoxic F_IO_2, we characterized CBF at 21% F_IO_2 and again during exposure to F_IO_2 between 30–100% at 1 atmosphere (atm). To determine whether hyperoxia-induced reductions in CBF are transient or sustained, we also measured CBF following cessation of 100% F_IO_2 as each subject was returned to 21% F_IO_2. To achieve those objectives, we enrolled 26 adult subjects; 13 were randomized into Arm 1 and exposed to 21%, 30%, 40%, 50%, and 100% F_IO_2, followed by 21% F_IO_2. The remaining 13 subjects were randomized into Arm 2 and exposed to 21%, 60%, 70%, 80%, and 100% F_IO_2, followed by 21% F_IO_2. This enabled us to test the following hypotheses: 1) the neurovascular response to hyperoxia, manifest as a reduction in CBF, will exhibit a dose-response relationship; and 2) termination of 100% F_IO_2 followed by resumption of 21% F_IO_2 will be followed by a return of CBF to baseline levels.

METHODS

Subjects

The study protocol was approved in advance by the Naval Medical Research Unit-Dayton Institutional Review Board (protocol #NAMRUD.2020.0003). Reliance agreements were arranged with The Christ Hospital, Cincinnati, OH, USA, where the study took place, and with Case Western Reserve University. Each subject received a description of the protocol and provided written informed consent before participating. MRI eligibility screening was performed at the time of consent and again prior to MRI scanning to ensure subject safety.

Equipment/Materials

To assess the primary outcome measure of cerebral blood flow, subjects were placed within a 3T whole-body MR scanner (Magnetom Skyra; Siemens Healthcare, Erlangen, Germany) using the body coil for radio frequency transmission with a 20-channel receive-only phased-array head coil for reception. Anatomical MR images were first acquired using high resolution T1-weighted magnetization prepared rapid gradient echo (MPRAGE) imaging in the sagittal plane (TE/TR/TI: 2.32/2300/900 ms, flip angle: 8°; voxel size of 0.9 × 0.9 × 0.9 mm^3). Cerebral perfusion was detected using the Siemens pseudocontinuous arterial spin labeling (pCASL) sequence, which employs readout by 2D echo-planar imaging with background suppression. Imaging parameters were: TE = 17 ms, TR = 3600 ms, inversion time = 1800 ms, postlabeling delay = 1800 ms; 27 contiguous ascending slices with 4-mm slice thickness and 1-mm interslice spacing; FOV = 220 mm, imaging matrix = 64 × 64; and effective voxel size 3.4 × 3.4 × 4.00 mm. A perfusion-weighted image pair was obtained, followed by 20 alternating label and control images, for a total of 10 pCASL image pairs. An oxygen sensor (BIOPAC Systems®, Inc.; Goleta, CA, USA) was attached to the nonrebreather mask to validate inspired and expired oxygen levels and to continuously monitor respiratory rate.

Procedure

This study was conducted in Cincinnati, OH, located 147 m (~482 ft.) above sea level with an average barometric pressure of 747 mmHg. An overview of the study protocol is presented in **Fig. 1**. All subjects first received a physical examination with past medical history. Once placed onto the gantry of the MR scanner, foam pads were placed around the head to minimize movement and a nonrebreather mask (Salter Labs; Arvin, CA, USA) was placed over the subject's nose and mouth. A 30-foot, 3.0-mm bore tube connected the nonrebreather mask to the respiratory monitor described above.

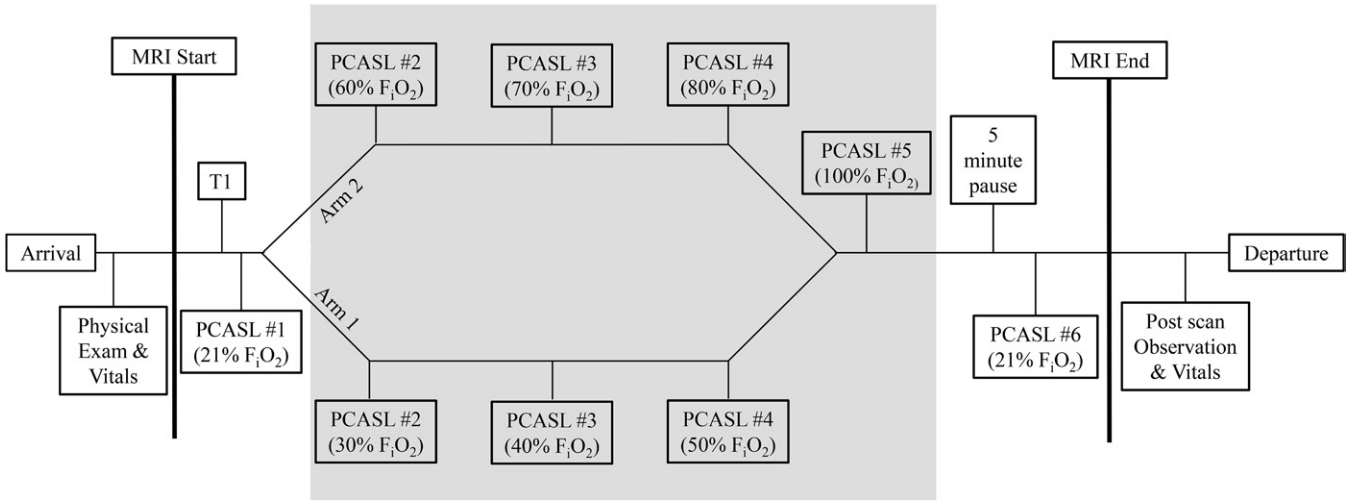

Fig. 1. Study overview. Gray shaded area represents hyperoxic exposure.

During the MR T1 anatomical scan, the nonrebreather mask delivered compressed room air (21% F_IO_2) to the subject. Upon completion of the anatomical scan, the following sequential steps were performed for subjects randomized to Arm 1:

1) the subject continued to breathe 21% F_IO_2 and baseline CBF was measured using pCASL;
2) F_IO_2 was increased to 30% and CBF was measured during pCASL #2;
3) F_IO_2 was increased to 40% and CBF was measured during pCASL #3;
4) F_IO_2 was increased to 50% and CBF was measured during pCASL #4;
5) F_IO_2 was increased to 100% and CBF was measured a fifth time, during pCASL #5; and
6) the subject was then returned to 21% F_IO_2 and, following a 5-min pause, the final pCASL sequence (#6) was acquired.

Those subjects randomized to Arm 2 received 60%, 70%, and 80% F_IO_2 during pCASL sequences #2–4, instead of 30%, 40%, and 50% F_IO_2 as described above for Arm 1 subjects.

Each pCASL sequence required 7 min to complete, with an interval between scans of 1–2 min to equilibrate both the MR system and the subject to the next dose of oxygen. Total time in the MR scanner was approximately 70 min; exposure time to hyperoxia was ~34 min. At the completion of all MRI scans, the subject was removed from the MR scanner, escorted back to the examination room, and observed for 30 min. Following a final assessment of vital signs, the subject was discharged from the study.

Statistical Analysis

Sample size estimation and power analyses were based on findings from our prior study,[1] with the intent to achieve a minimum statistical power of ≥ 0.80 at a two-tailed significance of < 0.05. Demographic characteristics of research subjects were summarized as mean, SD, and range for continuous variables and frequency and percentage for categorical variables. Physiological measures were continuous in nature and summarized with descriptive statistics, including the mean, SD, standard error of the mean (SEM), and range. Frequency analyses and normality plots provided data distributions. Comparisons of brain volumetric measures and cerebral perfusion at baseline and final between study arms were made using independent samples *t*-tests. Differences of cerebral perfusion from baseline at each F_IO_2 level in each arm were tested using paired *t*-tests. After testing the comparisons, the *P*-values were examined using the Bonferroni-Holm method for controlling the family-wise error rate related to multiple testing. All data are expressed as the mean ± 1 SD, unless otherwise indicated. Statistical analyses were performed using Statistical Package for Social Sciences (SPSS) version 28 (Armonk, NY, USA; IBM Corp.) and Statistical Analysis Software (SAS) version 9.4 (SAS Institute, Cary, NC, USA). All tests were two-sided, with $P < 0.05$ considered statistically significant.

MRI DICOM files were converted to NIFTI format using dcm2niix. Anatomical MPRAGE images were processed with an automated processing pipeline available in BrainSuite version 19b software.[8] This generated 3 dimensional models of each subject's brain, derived from the T1 MPRAGE, which define gray matter, white matter, ventricular, and sinus spaces. A reference atlas was morphed onto the segmented regions, followed by calculations of volumetric and surface thickness values for gray matter, white matter, and ventricles for 103 regions of interest (ROI) using SVReg.[5–7]

pCASL images were processed using a pipeline that was created from code available within the ASLtbx,[4,16] which employs MATLAB and SPM12. Briefly, the processing steps comprise motion correction, rejection of outlier images, coregistration of ASL images with the anatomical MPRAGE image, creation of a brain mask, filtering and smoothing, and computation of CBF.[11] To determine CBF in gray and white matter, tissue probability maps[15] were computed from the MPRAGE anatomical scan using the SPM12 "segmentation" function, and then transformed to the same resolution as the pCASL images. CBF values were assigned to a tissue category (gray or white matter) when the tissue probability of the voxel was > 75%. For CBF summarization per brain, the CBF map was resampled into the structural image space using trilinear interpolation, and CBF values averaged for each brain compartment. This provided values of CBF as milliliters per minute per 100 grams of tissue (ml/min/100 g). Processing was automated using Visual Basic for Applications code in a Microsoft Access database, which was also used to summarize all MRI data.

RESULTS

Key demographics of the 26 research subjects are presented in **Table I**. Arm 1 and Arm 2 groups did not differ significantly by age, BMI, or sex distribution.

Brain Volumetric Analysis

T1 MPRAGE scans were processed using BrainSuite[13] to provide volumetric measures of white matter, gray matter, and total volume (gray matter + white matter) of 103 specific brain ROIs. Volumes for each ROI were normalized by total brain volume prior to comparisons between subjects in Arm 1 (low oxygen exposure) and Arm 2 (high oxygen exposure) groups. No significant differences existed between Arm 1 and Arm 2 research subjects regarding total brain volume, nor any of the 103 brain

Table I. Subject Demographics.

	ARM 1: LOW F_IO_2	ARM 2: HIGH F_IO_2	*P**
Gender			
Male	6 (46%)	7 (54%)	0.69**
Female	7 (54%)	6 (46%)	
Age (yr)			
Mean (SD)	27.5 (7.7)	31.2 (10.3)	0.31
Range	22–52	22–54	
BMI (kg/m^2)			
Mean (SD)	30.2 (9.2)	25.5 (3.1)	0.10
Range	20.5–52.4	21.3–30.7	

*Independent samples *t*-test; **Chi-squared test, 2-tailed significance.

Table II. Cerebral Perfusion (CBF) by Group.

	ARM 1: LOW F_IO_2	ARM 2: HIGH F_IO_2	*P**
Baseline CBF @ 21% F_IO_2			
Mean (SD)	49.2(10.7)	46.2(10.1)	0.46
Range	27.5-69.3	30.2-61.6	
Final CBF @ 21% F_IO_2			
Mean (SD)	47.4(11.5)	44.8(9.9)	0.53
Range	22.3-68.0	29.3-58.3	

Comparisons of CBF values (ml/min/100 g) for subjects within Arm 1 and Arm 2 measured at baseline during exposure to 21% F_IO_2 and again at 21% F_IO_2 following hyperoxia.
*Independent samples *t*-test, 2-tailed significance.

regions of interest after Bonferroni-Holm correction for multiple testing.

Cerebral Perfusion at 21% F_IO_2

Baseline CBF at 21% F_IO_2 did not differ between subjects randomized to Arm 1 or Arm 2 (**Table II**) and are comparable to those previously measured with a Siemens 3T MR scanner using pulsed arterial spin labeling.[1,3] Following cessation of 100% F_IO_2 and resumption of 21% F_IO_2, CBF returned to levels similar to those measured at baseline.

Cerebral Perfusion During Low-Dose Hyperoxia

Exposure to low-dose F_IO_2 of 30%, 40%, and 50% did not affect CBF within subjects randomized to Arm 1 (**Table III**). When exposed to 100% F_IO_2, Arm 1 subjects experienced a significant reduction in CBF compared to baseline 21% F_IO_2 ($t = 8.36$, $df = 12$, $P < 0.001$, adjusted $P < 0.005$). That mean reduction of CBF (24.7% ± 10.0%) was similar to that observed in prior studies.[1,3]

Cerebral Perfusion During High-Dose Hyperoxia

Exposure to each high-dose F_IO_2 level evoked significant reductions ($P < 0.001$; adjusted $P < 0.005$) in CBF within subjects randomized to Arm 2 ($t = 5.04$, $df = 12$ at $F_IO_2 = 60\%$; $t = 7.21$, $df = 12$ at $F_IO_2 = 70\%$; $t = 9.57$, $df = 12$ at $F_IO_2 = 80\%$) (**Table IV**). When exposed to 100% F_IO_2, Arm 2 subjects experienced a mean reduction of 29.5% ± 7.3% in CBF compared to baseline 21% F_IO_2 ($t = 11.30$, $df = 12$, $P < 0.001$, adjusted $P < 0.005$), a reduction similar to that experienced by subjects within Arm 1. This reduction in CBF is consistent with observations in prior studies.[1,3]

Fig. 2 graphically illustrates side-by-side comparisons of CBF for both Arm 1 and Arm 2 subjects at each F_IO_2. Baseline CBF was the same for both Arm 1 and Arm 2 subjects and was unchanged following onset of hyperoxia between 30–50% F_IO_2 (Arm 1). In contrast, CBF values were markedly reduced below baseline by exposure to hyperoxia of 60–80% F_IO_2 (Arm 2). Fig. 2 also demonstrates that both Arm 1 and Arm 2 subjects experienced similar reductions in CBF during exposure to 100% F_IO_2, and that CBF returned to baseline levels when subjects were returned to 21% F_IO_2. **Fig. 3** presents representative pCASL images from two different subjects revealing changes in cerebral perfusion during low dose and high dose oxygen exposures.

Respiratory Frequency

Respiratory rate was continuously monitored in all subjects throughout each pCASL sequence. Respiratory rate was not obtained in one female subject in Arm 2 due to an occlusion in the sampling tube that developed during the scanning session. Breathing rates remained stable throughout all oxygen exposures for all subjects. No differences in respiratory rate were found between Arm 1 and Arm 2 subjects during exposures to 21% F_IO_2 (baseline pCASL #1 or at the final pCASL #6), nor during exposure to 100% F_IO_2. Additionally, respiratory frequency did not differ between men and women.

DISCUSSION

The primary objective for this study was to determine if a dose response relationship existed between F_IO_2 and CBF. We found that CBF was unaffected by low-dose $F_IO_2 \geq 30$ and $\leq 50\%$, but was significantly reduced during exposure to $F_IO_2 \geq 60\%$. We also observed that all subjects experienced reduced CBF during exposure to 100% F_IO_2. Cessation of 100% F_IO_2, followed by resumption of 21% F_IO_2, led to a restoration of CBF. Collectively, those findings suggest: 1) a dose-response relationship exists between F_IO_2 and CBF; 2) an $F_IO_2 \geq 60\%$ is the threshold at which CBF first becomes reduced; and 3) CBF is reduced only during exposure to hyperoxia and rebounds back to baseline upon cessation of the hyperoxic stimulus.

No difference in age, BMI, or sex distribution existed between subjects who were randomized into the low F_IO_2 group (Arm 1) or the high F_IO_2 group (Arm 2). Both groups showed similar prehyperoxia CBF values at 21% F_IO_2, as well as during exposure to 100% F_IO_2, and again during post-hyperoxia resumption of 21% F_IO_2. This suggests an absence of between-group systematic errors in data acquisition or processing that could account for the lack of CBF change during exposure to 30%, 40%, or 50% F_IO_2 within Arm 1 subjects (Fig. 3). Rather, we interpret the lack of change in CBF to suggest the neurovascular system may be unaffected by $P_aO_2 \geq 92$ mmHg and ≤ 295 mmHg, which is the range encountered by Arm 1 subjects during exposure to $F_IO_2 \geq 21\%$ and $\leq 50\%$ at 1 atm.

Table III. Cerebral Perfusion (CBF) Values for Arm 1 (Low Dose F_IO_2 Exposure).

	21% F_IO_2	30% F_IO_2	40% F_IO_2	50% F_IO_2	100% F_IO_2	21% F_IO_2
CBF (ml/min/100 g)						
Mean ± SD	49.23 ± 10.73	49.30 ± 12.42	47.89 ± 11.04	46.40 ± 10.82	36.98 ± 8.40	47.44 ± 11.52
Range	27.51-69.33	24.67-73.49	23.88-63.52	21.33-59.15	17.37-51.38	22.31-68.04
P	N/A	0.94	0.35	0.20	<0.001	0.20
Adjusted *P*-value*	N/A	0.94	0.80	0.80	<0.005	0.80

CBF values for subjects in Arm 1 measured at baseline during exposure to 21% F_IO_2, and again during exposure to each level of hyperoxia.
*Paired samples *t*-test compared to initial 21% F_IO_2, adjusted *P*-value after Bonferroni-Holm correction, 2-tailed significance.

Table IV. Cerebral Perfusion (CBF) Values for Arm 2 (High Dose F_IO_2 Exposure).

	21% F_IO_2	60% F_IO_2	70% F_IO_2	80% F_IO_2	100% F_IO_2	21% F_IO_2
CBF (ml/min/100 g)						
Mean ± SD	46.16 ± 10.11	40.68 ± 8.74	36.00 ± 7.51	34.58 ± 8.59	32.46 ± 7.24	44.76 ± 9.86
Range	30.16-61.64	27.10-56.40	22.45-46.07	21.89-48.63	19.83-44.47	29.27-58.25
P	N/A	<0.001	<0.001	<0.001	<0.001	0.27
Adjusted *P*-value*	N/A	<0.005	<0.005	<0.005	<0.005	0.27

CBF values for subjects in Arm 2 measured at baseline during exposure to 21% F_IO_2, and again during exposure to each level of hyperoxia.
*Paired samples *t*-test compared to initial 21% F_IO_2; adjusted *P*-value after Bonferroni-Holm correction, 2-tailed significance.

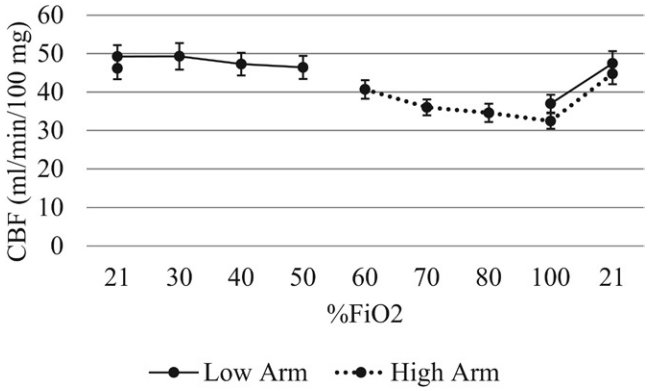

Fig. 2. Graphical representation of hyperoxia's effect on CBF. The figure illustrates similar baseline levels of CBF at 21% F_IO_2. Error bars represent SEM.

The alveolar gas equation predicts probable P_aO_2 values experienced by this study's subjects during their exposure to differing F_IO_2 concentrations.

$$P_AO_2 = F_IO_2\left(P_{ATM} - PH_2O\right) - \left[\frac{P_aCO_2}{R.Q.}\right]$$

Based upon this equation, an F_IO_2 of 60% delivered at a barometric pressure (P_{atm}) of 747 mmHg, in the presence of partial pressure of airway water vapor (PH_2O) of 47 mmHg, a partial pressure of arterial carbon dioxide (P_aCO_2) of 40 mmHg, and respiratory quotient (R.Q.) of 0.8 will yield a P_AO_2 of 370 mmHg. Accounting for an alveolar-arterial gradient of 5 mmHg, the expected P_aO_2 is 365 mmHg. Fig. 2 and Table IV suggest that at 1 atm, an F_IO_2 of 60% with a P_aO_2 of 365 mmHg evokes a significant reduction in CBF. Table IV, Fig. 2, and Fig. 3 also reveal that as F_IO_2 and P_aO_2 increased, CBF concomitantly decreased.

Our recent study demonstrated that 100% F_IO_2 reduced CBF by approximately 35%, which was accompanied by changes in cortical EEG activity and cognitive performance.[1] Findings from this current study suggest that an F_IO_2 of 60% at 1 ATM would induce a P_aO_2 of 365 mmHg, which appears to be the threshold at which reductions in CBF begin. However, aviators are exposed to lower barometric pressures; the most frequently encountered is 566 mmHg, which is equivalent to a cabin altitude of 8000 ft. At that barometric pressure, an F_IO_2 of 60% would provide a P_aO_2 of ~255 mmHg, which is well below the P_aO_2 of 365 mmHg that triggers a reduction in CBF. At a barometric pressure of 566 mmHg, an F_IO_2 of 80% would yield a P_aO_2 of 365 mmHg, and potentially, a reduction in CBF. This suggests the need to consider oxygen schedules providing F_IO_2 levels that are sufficient to reduce risks of hypobaric hypoxia and decompression injury, yet remain below the threshold that produces a reduction in CBF.

Respiratory frequency in the current sample did not decrease across exposures to hyperoxia. A previous report[1] noted respiratory rates dropped significantly for men when exposed to 100% F_IO_2, but only after 15 continuous minutes of hyperoxic

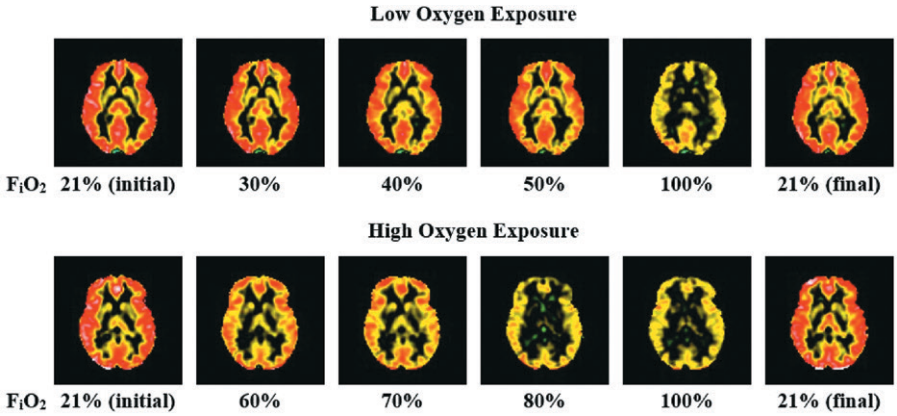

Fig. 3. Cerebral perfusion images acquired during low and high oxygen exposures. pCASL brain images are shown in the axial plane. Research subject exposure to F_IO_2 during image acquisition is located below each image. Yellow and red colors represent high cerebral perfusion (CBF) levels while black and green represent lower levels. The upper images were acquired from a representative individual within Arm 1 (low oxygen exposure). All images are at the same neuroanatomical location. The lower images were acquired from a representative individual within Arm 2 (high oxygen exposure). All images are at the approximate neuroanatomical location as seen in the upper images.

breathing. Hyperoxic exposures occurred in a stepwise progression in this protocol, with each F_IO_2 exposure limited to approximately 9 min. This may account for absence of change in respiratory frequency. Additionally, exposure to F_IO_2 levels under 100% may not evoke the same slowing of respiratory frequency.

We believe this to be the first study to characterize a dose-response relationship between F_IO_2 and CBF, and to establish that at 1 atm, an $F_IO_2 \geq 60\%$ may be the threshold at which CBF first becomes reduced. Additional strengths include equal distributions of age, BMI, and men and women within each study arm. Limitations to this study primarily were related to the COVID pandemic, which required minimal physical interactions between the study team and research subjects during all aspects of the study. This prohibited collection of ancillary data such as arterial blood gas samples or measures of cortical EEG, which may have provided novel insights into the physiological response of the pulmonary and central nervous systems to stepwise progressions in F_IO_2 and P_aO_2. However, the absence of those ancillary data had no impact upon acquisition and analyses of this study's primary outcome variable: the relationship between CBF and F_IO_2.

Findings from this study suggest that the neurovascular system's functional response to hyperoxia, manifest as a reduction in CBF, begins during exposure to $F_IO_2 \geq 60\%$ at 1 atm. There remains a need to establish whether reduction in CBF at $F_IO_2 \geq 60\%$ is also accompanied by similar changes in cortical EEG, cognitive performance, and autonomic function as was observed at an F_IO_2 of 100% at 1 atm.[1] In addition, defining the extent that hypobaric environments may attenuate 60% F_IO_2-induced reductions in CBF are needed to inform development of oxygen delivery schedules that confer maximal neuroprotection without concomitantly conferring risk of unintended brain hypoperfusion.

ACKNOWLEDGMENTS

Appreciation is extended to Matthew Roberts, MRI Technologist at The Christ Hospital Cincinnati, OH, for his assistance with MRI protocol development and image acquisition.

The views expressed in this paper reflect the results of research conducted by the author(s) and do not necessarily reflect the official policy or position of the Department of the Navy, Department of Defense, or the U.S. Government.

Financial Disclosure Statement: This work was supported by the Department of Defense, Naval Medical Research Center (N3239819P0321: MJD, EGD). The authors additionally are supported by the National Institutes of Health/National Institute of Nursing Research [R21NR017235: MJD, EGD], and the Department of Defense: 711th Human Performance Wing, U.S. Air Force School of Aerospace Medicine Studies & Analysis (20-010: M. J. Decker, E. G. Damato), and Air Force Research Laboratories (FA8650-19-C-6103: M. J. Decker). The authors have no competing interests to declare.

Authors and Affiliations: Elizabeth G. Damato, Ph.D., Naval Medical Research Unit-Dayton, Dayton, OH, and School of Nursing, Case Western Reserve University, Cleveland, OH, USA; Seth J. Fillioe, Ph.D., and Ian S. Vannix, M.S., Center for Aerospace Physiology, Department of Physiology and Biophysics, and Seunghee P. Margevicius, Ph.D., Department of Population and Quantitative Health Sciences, Case Western Reserve University School of Medicine, Cleveland, OH, USA; Lily K. Norton, M.S., Jacobs School of Medicine and Biomedical Sciences, University at Buffalo, Buffalo, NY, USA; and Jessica L. Beebe, D.O., The Wright Center Graduate Medical Education, HealthSource of Ohio, New Richmond, OH, USA, and Michael J. Decker, Naval Medical Research Unit-Dayton, Dayton, OH, and Center for Aerospace Physiology, Department of Physiology and Biophysics, Case Western Reserve University, Cleveland, OH, USA.

REFERENCES

1. Damato EG, Flak TA, Mayes RS, Strohl KP, Ziganti AM, et al. Neurovascular and cortical responses to hyperoxia: enhanced cognition and electroencephalographic activity despite reduced perfusion. J Physiol. 2020; 598(18):3941–3956.
2. Deussing EC, Artino AR Jr, Folga RV. In-flight hypoxia events in tactical jet aviation: characteristics compared to normobaric training. Aviat Space Environ Med. 2011; 82(8):775–781.
3. Floyd TF, Clark JM, Gelfand R, Detre JA, Ratcliffe S, et al. Independent cerebral vasoconstrictive effects of hyperoxia and accompanying arterial hypocapnia at 1 ATA. J Appl Physiol (1985). 2003; 95(6):2453–2461.
4. Hu WT, Wang Z, Lee VM, Trojanowski JQ, Detre JA, Grossman M. Distinct cerebral perfusion patterns in FTLD and AD. Neurology. 2010; 75(10):881–888.
5. Joshi AA, Shattuck DW, Leahy RM. A method for automated cortical surface registration and labeling. In: Dawant BM, Christensen GE, Fitzpatrick JM, Rueckert D, editors. Biomedical Image Registration. 5th International Workshop; July 7–8, 2012; Nashville, TN. Berlin: Springer; 2012:180–189.
6. Joshi AA, Shattuck DW, Thompson PM, Leahy RM. Cortical surface parameterization by p-harmonic energy minimization. Proc IEEE Int Symp Biomed Imaging. 2004; 1:428–431.
7. Joshi AA, Shattuck DW, Thompson PM, Leahy RM. Surface-constrained volumetric brain registration using harmonic mappings. IEEE Trans Med Imaging. 2007; 26(12):1657–1669.
8. Kazemi K, Noorizadeh N. Quantitative comparison of SPM, FSL, and Brainsuite for brain MR image segmentation. J Biomed Phys Eng. 2014; 4(1):13–26.
9. Lambertsen CJ, Dough RH, Cooper DY, Emmel GL, Loeschcke HH, Schmidt CF. Oxygen toxicity: effects in man of oxygen inhalation at 1 and 3.5 atmospheres upon blood gas transport, cerebral circulation and cerebral metabolism. J Appl Physiol. 1953; 5(9):471–486.
10. Leeuwis AE, Smith LA, Melbourne A, Hughes AD, Richards M, et al. Cerebral blood flow and cognitive functioning in a community-based, multi-ethnic cohort: The Sabre Study. Front Aging Neurosci. 2018; 10:279.
11. Li Y, Dolui S, Xie DF, Wang Z. Priors-guided slice-wise adaptive outlier cleaning for arterial spin labeling perfusion MRI. J Neurosci Methods. 2018; 307:248–253.
12. Paul AL, Ferl RJ. The biology of low atmospheric pressure: implications for exploration mission design and advanced life support. Gravit Space Biol 2006; 19(1):3–18.
13. Shattuck DW, Leahy RM. BrainSuite: an automated cortical surface identification tool. Med Image Anal. 2002; 6(2):129–142.
14. Smith A. Hypoxia symptoms reported during helicopter operations below 10,000 ft: a retrospective survey. Aviat Space Environ Med. 2005; 76(8):794–798.
15. Wang R, Li C, Wang J, Wei X, Li Y, et al. Automatic segmentation and quantitative analysis of white matter hyperintensities on FLAIR images using trimmed-likelihood estimator. Acad Radiol. 2014; 21(12):1512–1523.
16. Wang Z, Aguirre GK, Rao H, Wang J, Fernández-Seara MA, et al. Empirical optimization of ASL data analysis using an ASL data processing toolbox: ASLtbx. Magn Reson Imaging. 2008; 26(2):261–269.
17. West JB. A strategy for in-flight measurements of physiology of pilots of high-performance fighter aircraft. J Appl Physiol (1985). 2013; 115(1):145–149.
18. Woodrow AD, Webb JT, Wier GS. Recollection of hypoxia symptoms between training events. Aviat Space Environ Med. 2011; 82(12): 1143–1147.